Optical transition energies for lead-salt semiconductor quantum wells

Erasmo A. de Andrada e Silva
Instituto Nacional de Pesquisas Espaciais–INPE, Caixa Postal 515, 12201 São José dos Campos, SP, Brazil
(Received 22 March 1999)

The quantized states for electrons and holes confined in lead-salt semiconductor quantum wells (QW's) grown on (100) and (111) substrates and the corresponding electric-dipole optical transition energies are calculated analytically, within the envelope function approximation and with the Dimmock two-band $\vec{k}\cdot\vec{p}$ model for the bulk. The solution takes into account nonparabolicity, anisotropy, and break of valley and spin degeneracy, due to quantum confinement. Transition energies for different PbTe QW's, calculated as a function of temperature and well width, are shown to give a fair description of the observations of the quantum size effect reported in the literature. Limitations of the spherical and of the parabolic approximations to the electronic structure of the lead-salt QW's are made clear and the Rashba spin-orbit term in the effective Hamiltonian is derived. [S0163-1829(99)03332-9]

I. INTRODUCTION

There is an increasing interest in the understanding of the unusual properties of the ten valence-electron IV-VI semiconductor compounds now that molecular-beam epitaxy (MBE) machines in different laboratories are dedicated to the growth of their thin films and heterostructures. The so-called lead salts (PbTe, PbSe, and PbS) form the most homogeneous and studied family of IV-VI compounds. They are narrow gap semiconductors used in the fabrication of infrared lasers and detectors, crystallize in the rocksalt cubic structure, and present similar energy bands. The small and fourfold degenerate direct gap ($\sim$0.2 eV) occurs at the edge of the Brillouin zone along the [111] direction (L point). Among their uncommon properties we recall the self-doping by deviation from stoichiometry, the ferroelectric tendency associated with the high static dielectric constant, and the increase of the gap with temperature, as opposed to all III-V and II-VI semiconductor compounds.[1] Their ternary alloys have been very important in the modulation of their properties, such as, for instance, the energy gap, and in different applications. The $Pb_{1-x}Sn_xTe$ compound and, more recently, the larger gap and diluted magnetic $Pb_{1-x}Eu_xTe$,[2] have been of particular importance in the fabrication of PbTe quantum wells (QW's).

Following the advances in semiconductor physics, the epitaxial growth of good quality lead-salt thin layers, QW's, and superlattices has contributed to a better understanding of the properties of these materials and to the improvement of their devices, especially high-temperature infrared lasers.[3] However, there are important electronic properties of these new heterostructures, like, for example, the heterojunction band offsets, the control of defects and carrier concentration, and the optical spectra, that deserve more investigation. This work reports the results of our theoretical investigation on the electronic structure and optical properties of the lead-salt QW's.

Infrared optical absorption measurements on multiple $PbTe/Pb_{1-x}Eu_xTe$ QW's have shown clear signs of quantum confinement. Ishida *et al.*[4] have studied wells grown on KCl (100) substrates and have obtained an absorption spectrum with regular steps corresponding to a uniform series of transition energies between quantized electron and hole states. More recently Yuan *et al.*[5] performed similar measurements on similar structures grown on BaF_2 (111) substrates and have observed a more complicated frequency dependence of the absorption coefficient, due to the presence of two series of quantized states from nonequivalent valleys. Size quantization effects were also clearly seen in the luminescence response of other lead-salt QW's.[6–8]

The observed spectra have been shown to be in good agreement with the transition energies calculated within the envelope function approximation.[9] However, the numerical calculation is a difficult one, not easily reproducible, and depends on a not well controlled approximation for the envelope function boundary conditions. An envelope function solution for the problem of calculating the electronic states of lead-salt QW's with none of the above disadvantages is presented here. It is based on the semiempirical anisotropic two-band Kane-like $\vec{k}\cdot\vec{p}$ model for the bulk, proposed by Dimmock,[10] and presents analytical solutions for the QW subband structure.[11,12] The model is solved for QW's grown along both [100] and [111] directions and is shown to give a simple and quite accurate description of the available data. In Sec. II we introduce the model for both bulk and QW. In Sec. III we present the results for the optical transition energies of different PbTe QW's as a function of temperature and well width and compare with the experiments. Finally in the last section we summarize the main results and conclusions.

II. MODEL

The electronic wave functions in the effective mass or envelope function approximation are given by sums of products of Bloch functions at the band-edge point of the Brillouin zone (BZ) and slowly varying envelope functions.[13] For the QW, the allowed energy levels and the envelope functions satisfy an eigenvalue problem with the effective Hamiltonian for the bulk plus appropriate boundary conditions at the interfaces.

TABLE I. Low-temperature conduction and valence band-edge effective masses [both longitudinal (along [111]) and transverse] in units of free electron mass, and the fundamental band gap of the three lead salts, obtained via oscillatory magnetoresistance, cyclotron resonance, and refractive index measurements (Ref. 1).

	PbTe	PbSe	PbS
$m_{\parallel}^{e}$	0.240	0.070	0.105
$m_{\perp}^{e}$	0.024	0.040	0.080
$m_{\parallel}^{h}$	0.310	0.068	0.105
$m_{\perp}^{h}$	0.022	0.034	0.075
E_g (eV)	0.19	0.15	0.29

A. Bulk

In the case of the lead salts one of the simplest models, represented by the Kane-like $\vec{k}\cdot\vec{p}$ Hamiltonian around the L point of the BZ, can be written as[10]

$$H=\begin{pmatrix} \frac{E_g}{2} & 0 & P_{\parallel}k_{\parallel} & P_{\perp}k_{\perp} \\ 0 & \frac{E_g}{2} & P_{\perp}k_{\perp} & -P_{\parallel}k_{\parallel} \\ P_{\parallel}k_{\parallel} & P_{\perp}k_{\perp} & -\frac{E_g}{2} & 0 \\ P_{\perp}k_{\perp} & -P_{\parallel}k_{\parallel} & 0 & -\frac{E_g}{2} \end{pmatrix}, \qquad (1)$$

where E_g stands for the band gap, $P_{\parallel}$ and $P_{\perp}$ are the longitudinal (along [111]) and perpendicular momentum interband matrix elements, and the coordinate axes are such that the electron wave vector measured from the L point is written as $\mathbf{k}=(k_1,k_2,k_3)=(k_{\perp},0,k_{\parallel})$. The upper and lower blocks correspond to the spin degenerate L_6^- conduction and L_6^+ valence bands, respectively. The free electron kinetic energy in the diagonal has been neglected as is usually done in view of the smallness of the effective mass, which is determined mainly by the off-diagonal elements and in view of important simplifications due to linearity in k.

The resulting dispersion relation corresponds to spin degenerate, specular symmetric, nonparabolic, and anisotropic conduction and valence bands, which can be written as

$$E=\pm\frac{E_g}{2}\pm\frac{\hbar^2}{2}\left(\frac{k_{\parallel}^2}{m_{\parallel}(E)}+\frac{k_{\perp}^2}{m_{\perp}(E)}\right), \qquad (2)$$

where the upper sign is used for the conduction band ($E>E_g/2$) and the lower one for the valence band ($E<-E_g/2$), and the energy dependent effective masses, describing the nonparabolicity of the bands, are given by $m_{\parallel,\perp}(E)=(\hbar^2/2P_{\parallel,\perp}^2)(|E|+E_g/2)$. In this model electrons and holes have exactly the same mass. We have listed in Table I the low-temperature longitudinal and transverse effective masses for electrons and holes in the different lead salts. One sees that the real band structure of these materials, near the fundamental gap, is in fact almost specular.

The difference between the effective mass of the electron and that of the hole is usually taken care of by including interactions with far bands, via perturbation theory. However, besides introducing new parameters, it leads to undesirable k^2 terms in the matrix elements. We here propose instead the use of the above two-band model with two different sets of effective momentum matrix elements $\{P_{\parallel}^{e},P_{\perp}^{e}\}$ and $\{P_{\parallel}^{h},P_{\perp}^{h}\}$ to calculate independently the electron and the hole quantized states. The effective matrix elements are those that reproduce the experimentally determined band-edge effective masses $m_{\parallel,\perp}^{e,h}(0)$ listed in Table I, i.e., $P_{\parallel,\perp}^{e,h}=\hbar^2E_g/2m_{\parallel,\perp}^{e,h}(0)$.

Doing so the simpler Dirac form of the effective Hamiltonian in the two-band approximation, which is amenable to heterostructure calculations,[15] is preserved while all major quantitative features of the lead-salt-bulk band structure near the fundamental gap are taken into account. With such a model for the bulk the QW problem in the zero bias and flat band conditions can be solved analytically.

B. Quantum well

The fabrication of good quality PbTe QW's (the most studied lead-salt QW) has been possible to a good extent due to the smaller and the larger energy gap of $Pb_{1-x}Sn_xTe$ and $Pb_{1-x}Eu_xTe$ alloys, respectively. For small concentrations x of Sn and Eu these alloys present crystal structure and lattice constant very close to pure PbTe. This fact is the basis of the applicability of the envelope function approximation to the QW problem and allows the interband momentum matrix elements to be considered the same for both well and barrier materials. In fact, for small x it is a good approximation to assume the energy gap as the only parameter in the $\vec{k}\cdot\vec{p}$ model that depends on composition and on temperature.[10,16] This is the main assumption of the envelope function approximation and of the present calculation.

The quantized energy levels for the confined electrons and holes are obtained with the solution of the eigenvalue problem with the effective Hamiltonian, which is given by that of the bulk [Eq. (1)] with the band gap varying along the growth direction, k_i $(i=1,2,3)$ substituted by $-id/dx_i$, and the band-edge discontinuities added to the diagonal element according to the band offset. The mathematical problem corresponds to that of four coupled first order differential equations for the four envelope function components. Using the appropriate effective momentum matrix elements we will, as discussed above, calculate first the electron states and then those for the holes. It is then natural to use two of the equations in order to eliminate the envelope function components of the other band and obtain a Schrödinger-like (second order) equation for the components of the band we are interested in. Such a projection procedure of the effective Hamiltonian into the conduction band, for example, results in

$$H_{2\times2}F_c=[h_c+h_{vc}(E-h_v)^{-1}h_{cv}]F_c=EF_c, \qquad (3)$$

where $F_c=(f^{\uparrow},f^{\downarrow})$ is the conduction band envelope function spinor with a component for each spin orientation, the h_c, h_v, h_{cv}, and h_{vc} are 2×2 matrix operators, and E is the electron energy. Such an effective Hamiltonian $H_{2\times2}$ depends on the growth direction, which can be oriented differently with respect to the longitudinal direction of the different nonequivalent valleys, breaking the valley degeneracy.

In lead-salt QW's grown along the [111] direction, for example, the four valleys are split into one longitudinal, with

the larger effective mass along the growth direction and lower confining energies, and three oblique ones, that have their longitudinal direction making with the growth direction an angle $\theta=\cos^{-1}(\frac{1}{3})$. Therefore, one obtains from the bulk Hamiltonian $H_{2\times2}$ in Eq. (3) two effective Hamiltonians, $H^l_{2\times2}$ for the longitudinal valley and $H^o_{2\times2}$ for the oblique one. The first can be easily found, while $H^o_{2\times2}$ is obtained after an appropriate rotation of the coordinate axis, leaving the growth direction fixed.

For the longitudinal valley one can set in the bulk Hamiltonian [Eq. (1)] $(x_1,x_2,x_3)=(x,y,z)$, where the z axis, along [111], is parallel to the growth direction and x,y are two orthogonal transverse directions, and obtain $h_c=[E_g(z)/2+Q(z)]I$, $h_v=[-E_g(z)/2+Q(z)]I$, and

$$h_{cv}=h_{vc}=-i\begin{pmatrix} P_\parallel\dfrac{d}{dz} & P_\perp\left(\dfrac{d}{dx}-i\dfrac{d}{dy}\right)\\ P_\perp\left(\dfrac{d}{dx}+i\dfrac{d}{dy}\right) & -P_\parallel\dfrac{d}{dz}\end{pmatrix},$$

where I is the 2×2 unit matrix and $Q(z)$ is a step function that sets the position of the center of the gap along the growth direction. Performing now the matrix products in Eq. (3) we get the following effective Hamiltonian:

$$H^l_{2\times2}=\left(-\frac{\hbar^2}{2}\frac{d}{dz}\frac{1}{m_\parallel}\frac{d}{dz}+\frac{\hbar^2k_\perp^2}{2m_\perp}+\frac{E_g}{2}+Q\right)I+\alpha_{\rm so}\boldsymbol{\sigma}\times\mathbf{k}_\perp\cdot\hat{z}, \tag{4}$$

where

$$m_{\parallel,\perp}=m_{\parallel,\perp}(z,E)=\frac{\hbar^2}{2P^2_{\parallel,\perp}}\left(E+\frac{E_g(z)}{2}-Q(z)\right), \tag{5}$$

$$\alpha_{\rm so}=\alpha_{\rm so}(z,E)=P_\parallel P_\perp\frac{d}{dz}\left(\frac{1}{E+E_g(z)/2-Q(z)}\right), \tag{6}$$

and $\vec{\sigma}$ is the vector of the Pauli spin matrices.

The off-diagonal elements correspond to the so-called Rashba spin-orbit term $(\alpha_{\rm so}\boldsymbol{\sigma}\times\mathbf{k}_\perp\cdot\hat{z})$. Note that this term is zero for $k_\perp=0$ and in each piece of semiconductor, where $E_g(z)$ and $Q(z)$ are constant. As in the case of the III-V QW's, this term leads to spin dependent boundary conditions for the states with $k_\perp\neq0$.[14] Spin-orbit splittings in both conduction and valence subbands of lead-salt asymmetric QW's are expected to be bigger than in corresponding III-V structures. We will here, however, limit ourselves to the problem of the optical transition energies of symmetric QW's. The complete subband structure of a general lead-salt QW and the effects of the Rashba spin-orbit term will be considered elsewhere.

The quantized energy levels in symmetric square QW's are spin degenerate and satisfy the following Schröndinger-like equation:

$$H^l(\varepsilon^l_n)f_n=\left(-\frac{\hbar^2}{2}\frac{d}{dz}\frac{1}{m_\parallel(z,\varepsilon^l_n)}\frac{d}{dz}+\frac{\hbar^2k_\perp^2}{2m_\perp(z,\varepsilon^l_n)}+V(z)\right)f_n=\varepsilon^l_nf_n, \tag{7}$$

TABLE II. Two-band effective masses for each nonequivalent valley, to be used in the calculation of the quantized subbands in lead-salt quantum wells grown along [111] and [100].

	m_1	m_2	m_3	Valley (n_v)
[111]	$m_\parallel$	$m_\perp$	$m_\perp$	$l(1)$
	$9m_\parallel m_\perp/(8m_\parallel+m_\perp)$	$m_\perp$	$(8m_\parallel+m_\perp)/9$	$o(3)$
[100]	$3m_\parallel m_\perp/(2m_\parallel+m_\perp)$	$m_\perp$	$(2m_\parallel+m_\perp)/3$	$o(4)$

where $V(z)=E_c(z)=E_g(z)/2+Q(z)$ gives then the conduction band edge modulation along the growth direction and $\varepsilon^l_n(\mathbf{k}_\perp)$, $n=1,2,3,\ldots$ are the longitudinal valley subbands.

Finally, to obtain the equation for the oblique valleys, we take $\hat{x}$ as the rotation axis and perform the above mentioned rotation, i.e., calculate $H^o_{2\times2}=T_\theta H_{2\times2}T_\theta^{-1}$ with

$$T_\theta=\begin{pmatrix}\cos\left(\dfrac{\theta}{2}\right) & i\sin\left(\dfrac{\theta}{2}\right)\\ i\sin\left(\dfrac{\theta}{2}\right) & \cos\left(\dfrac{\theta}{2}\right)\end{pmatrix}, \tag{8}$$

and substitute $\mathbf{k}$ by $(k_x,k_y\cos\theta-k_z\sin\theta,\ k_y\sin\theta+k_z\cos\theta)$ (see also Ref. 17). After some simple algebra one can write

$$H^o(\varepsilon^o_n)=-\frac{\hbar^2}{2}\frac{d}{dz}\frac{1}{m_1(z,\varepsilon^o_n)}\frac{d}{dz}+\frac{\hbar^2k_x^2}{2m_2(z,\varepsilon^o_n)}+\frac{\hbar^2k_y^2}{2m_3(z,\varepsilon^o_n)}+V(z), \tag{9}$$

where m_1, m_2, and m_3 are the combinations listed in Table II of the energy dependent longitudinal and transverse effective masses. The same equation, with the m_i also listed in Table II, is obtained in the case of (100) QW's where all four valleys are still degenerate but all oblique. Similar results were first obtained by Stern and Howard[18] in the context of n-type Ge-inversion layers. However, contrary to Ge, the lead salts are direct narrow gap semiconductors, with quasispecular nonparabolic conduction and valence bands. The present work extends the results of Ref. 18 by including the valence band and the nonparabolicity effects.

The solution for the quantized levels is now straightforward. Neglecting any band bending in view of the high static dielectric constant, we can write plane wave solutions in each piece of bulk with wave vectors $q=\pm\sqrt{(2m_{1,w}/\hbar^2)(\varepsilon-V_w)}$ and $\chi=\pm\sqrt{(2m_{1,b}/\hbar^2)(V_b-\varepsilon)}$ in the well and in the barrier, respectively. By matching the solutions at the interface, using the Ben Daniel-Duke-like boundary conditions one gets for $k_\perp=0$, we obtain the usual implicit equations:

$$\frac{\chi}{m_{1,b}}=\frac{q}{m_{1,w}}\tan\left(\frac{qL}{2}\right) \tag{10}$$

and

$$\frac{\chi}{m_{1,b}}=-\frac{q}{m_{1,w}}\cot\left(\frac{qL}{2}\right), \tag{11}$$

for the even and odd solutions, respectively, where L is the well width. These equations are satisfied by the allowed energy levels and are equivalent to the expressions obtained

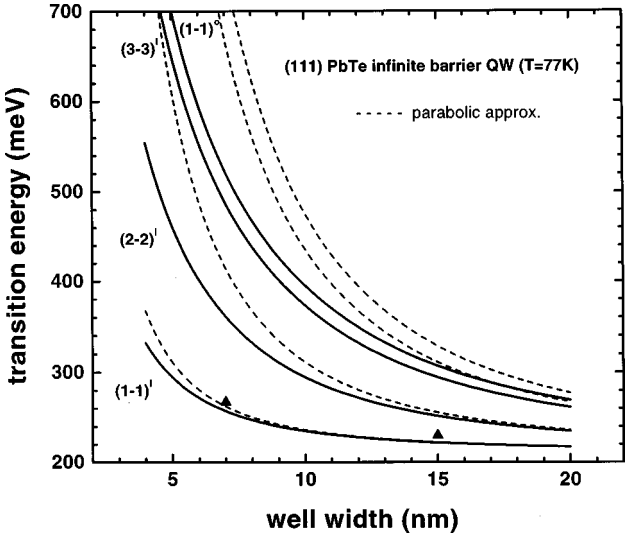

FIG. 1. Optical transition energies calculated for [111] infinite barrier PbTe QW's as a function of well width and for a temperature of 77 K. The transitions are labeled according to the corresponding valley (l for longitudinal and o for oblique) and quantized level (1,2,3, . . .). The dashed lines give the parabolic approximation and the triangles represent the luminescence data obtained by Zasavitskii *et al.* (Ref. 8) with $PbTe/BaF_2$ multiple QW's.

before with the same model, except for the effective momentum matrix elements.[11,12] They differ from those for simple III-V QW's mainly by the energy dependent effective mass and by the different series of quantized levels corresponding to nonequivalent valleys. In the next section we discuss the results for the electric-dipole optical transition energies, which are denoted and given by $E_{(n-n)^i}=E_g+\varepsilon^i_{e,n}(\mathbf{k}_\perp=0)+\varepsilon^i_{h,n}(\mathbf{k}_\perp=0)$, where $i=l$ (longitudinal) or o (oblique) indicates the corresponding valley and $\varepsilon^i_{e,n}$ and $\varepsilon^i_{h,n}$, the electron and hole quantized levels with $n=1,2,\ldots$, are both positive and measured from the respective band edge.

III. RESULTS

The optical properties of different PbTe QW's have been investigated by different groups with different methods. Here we discuss the validity and utility of the above model comparing its results with the available data of three types of QW's.

A. Infinite barrier PbTe QW

As an example of the application of the above theory, we have calculated the optical transition energies for infinite barrier [111] and [100] PbTe QW's. Besides illustrating the effects of the quantum confinement in lead-salt QW's, this example is useful in the interpretation of the optical spectrum of MBE grown $PbTe/BaF_2$ multiple quantum well (MQW) structures.[8] In Fig. 1 we have plotted the transition energies at a temperature of 77 K and as a function of the [111] well width.[20] It is interesting to note that due to the strong confinement, below the first transition from the oblique valleys $[(1-1)^o]$ we find three transitions from the longitudinal valley. The dashed lines give the parabolic approximation, which is seen to overestimate the transition energies especially in the case of narrow wells and excited states. In Fig. 1 we also compare the present model with recent measurements of the luminescence response from two good quality $PbTe/BaF_2$ MQW samples.[8]

Depending on the material combinations and the growth conditions of the sample, there can be other contributions to the shift (with respect to the bulk band gap) observed in the transition energies of these nanostructures. The strain-stress contribution, in particular, is of general importance for a complete interpretation of the data. In order to include it, all one has to do is to correct the input bulk band gaps; the calculation procedure described above remains the same. However, besides depending on the sample and the growth conditions, the estimation of such a shift requires knowledge of the deformation potential, which for these materials is not well known.[7,9] The results we present here contain only the quantum size shift, which is the dominant one in the case of thin QW's. The study of corrections from, for instance, many-body effects, dielectric confinement,[19] or strain-stress effects is outside the scope of this paper.

We have looked also at the temperature dependence of the optical transition energies. In Fig. 2 we have plotted it for a 10 nm wide PbTe infinite barier QW grown along both [111] and [100] directions. Note that the effect of increasing transition energy with temperature is much less pronounced in the case of (100) QW's due to the smaller effective mass along the growth direction. It is also important to note that the parabolic approximation gives misleading temperature dependence of the transition energies, in particular, for the oblique valleys.

B. $PbTe/Pb_{1-x}Eu_xTe$ QW's

The lead-salt QW that has been most studied is, however, the $PbTe/Pb_{1-x}Eu_xTe$. The quartenary PbEuTeSe compound has also been used as barrier material with smaller lattice mismatch. The quantum Hall effect,[22] the luminescence response,[6] and the magnetoreflectivity[23] of MQW's of this type have been investigated. However, a more direct observation of the confined states was obtained with optical absorption measurements, which also probe the excited energy levels. Ishida *et al.*[4] have studied, at room temperature, a series of samples with 5% of Eu, with varying PbTe well width and grown on top of KCl (100) substrates. Figure 3 compares their results with the present theory. The error bars simply indicate uncertainties in the experimental values, which includes also the well width determination and which in a rough estimation was taken here as of the order of the absorption step width.

In view of the limitations of both theory and experiment, one can say from Fig. 3 that the present simplified model gives a reasonable description of the well width dependence of the optical transition energies of these QW's, including the excited levels. Besides the missing contribution from strain-stress effects, which depends on the kind of the valley, one should remember that the higher the energy level, the less accurate is the model, due to the bigger importance of the k^2 terms neglected in the Hamiltonian. We have calculated the transition energies assuming a type I band alignment and with different values of the band offset (defined as $Q=\Delta E_c/\Delta E_g$). The agreement obtained in Fig. 3 (with Q

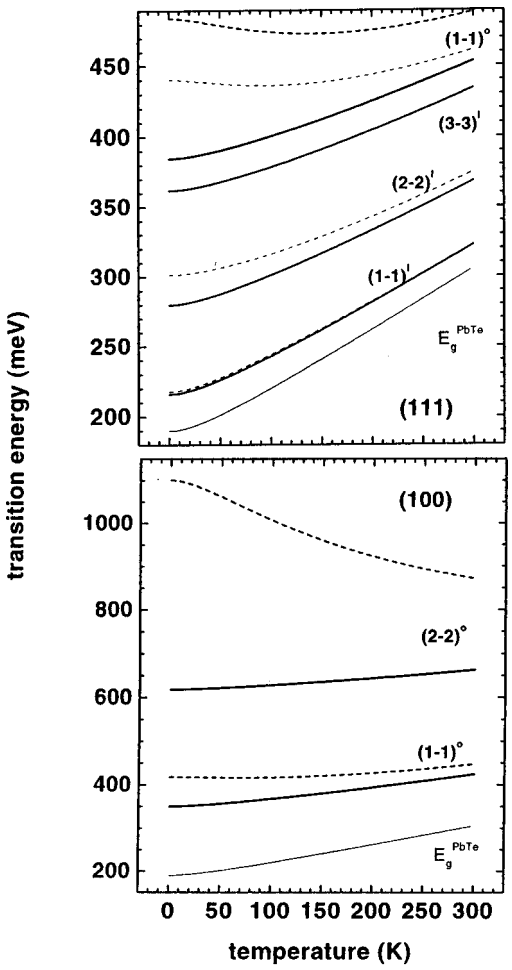

FIG. 2. Temperature dependence of the transition energies in infinite barrier PbTe QW's with $L=10$ nm and grown along the directions [111] and [100]. Note that in the (100) QW all valleys are degenerate and oblique. The dashed lines show the poor performance of the parabolic approximation in the description of the temperature dependence. The bulk PbTe band gap is also shown.

$=0.5$) is, however, practically independent of the band offset, due to the strong confinement and the almost specular symmetry between the conduction and valence bands.

The transmission spectra of $PbTe/Pb_{1-x}Eu_xTe$ MQW's grown along the [111] direction have been investigated by Yuan *et al.*[5] They have measured the optical absorption of three samples at temperatures of 5 and 77 K, but all with a different concentration of Eu and PbTe well width. In Fig. 4 we compare the results of our model calculation with the transition energies obtained for one of the samples. Again we see some discrepancies, which need to be investigated further, but one can still say that the model gives a reasonable prediction of the position of the absorption steps. Similar agreements were obtained with the other two samples as well.

C. $Pb_{1-x}Sn_xTe/PbTe$ QW's

As the last example we consider the quantum size effect in $Pb_{1-x}Sn_xTe/PbTe$ QW's. Multiple wide QW's of $Pb_{1-x}Sn_xTe/PbTe$ have been studied both theoretically and experimentally by Kriechbaum *et al.*[9] However, we here

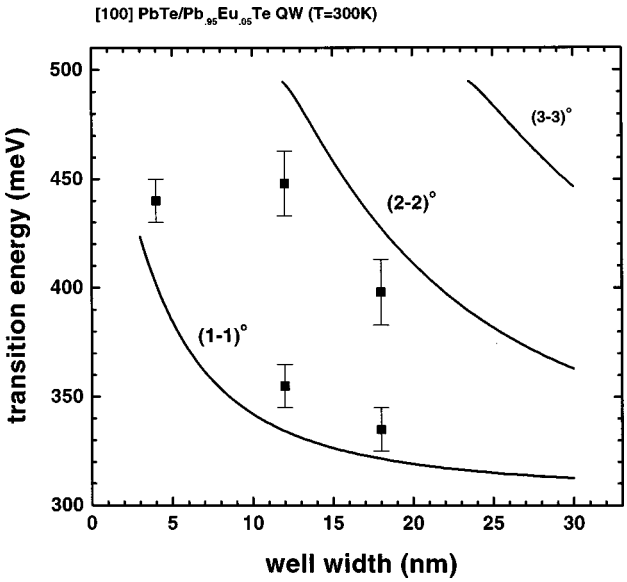

FIG. 3. Comparison of the transition energies calculated here with those obtained by Ishida *et al.* (Ref. 4) from the transmission spectra of (100) $PbTe/Pb_{0.95}Eu_{0.05}Te$ QW's, with varying well width. See text for the discussion.

show results in the thin QW limit and compare them with recent absorption measurements done at varying temperature and with a good quality MBE grown (111) sample, with 50 periods of 43 Å of $Pb_{0.75}Sn_{0.15}Te$ (well) and 424 Å of PbTe (barrier).[21] The transition energies at $T=150$ K are plotted in Fig. 5 as a function of the well width. The results of the calculation with three different band offsets are shown. These thin and shallow quantum wells ($\Delta E_c \sim 40$ meV) present only one bound state for each valley and are more sensitive to the value of the band offset. The positions of the

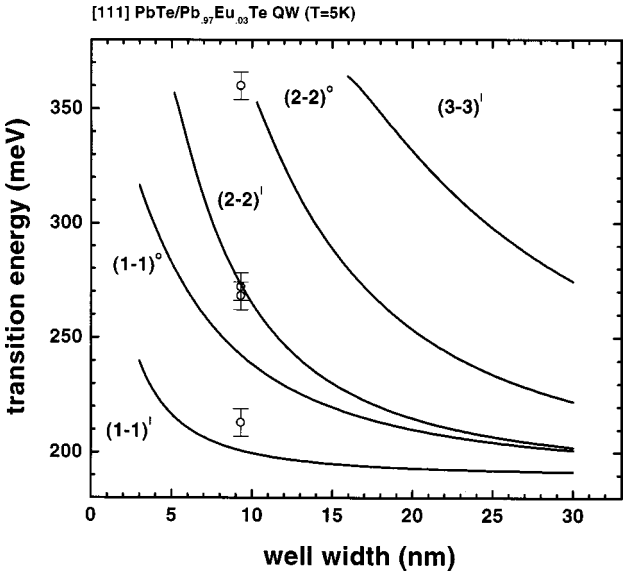

FIG. 4. Transition energies as a function of the well width for the case of (111) $PbTe/Pb_{0.93}Eu_{0.03}Te$ QW's. A band offset of 0.5 was used in the calculations. The experimental points correspond to the transition energies obtained from the transmission spectra by Yuan *et al.* (Ref. 5) and the error bars represent a rough estimation of the uncertainties.

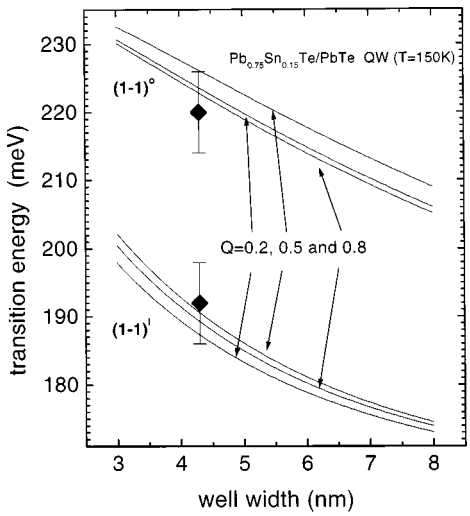

FIG. 5. Transition energies calculated as a function of the well width for the case of a (111) $Pb_{0.85}Sn_{0.15}Te/PbTe$ QW, with different band offsets. The figure also shows the position of the absorption steps recently observed by Rappl *et al.* (Ref. 21) in the spectrum of a good quality MBE gown multiple thin QW sample.

absorption steps observed experimentally and shown in the figure are well reproduced by the present model calculation, which indicates that these materials do indeed form a type I QW.[9] However, it is not possible to extract any conclusion with respect to the exact band offset. New measurements with a larger number of samples are necessary for a better understanding of the confining effects in these QW's. Finally it is worthwhile to mention that the temperature dependence of the transition energies up to room temperature was both measured and calculated and in both experiment and theory an almost linear increase (following the band gap) was obtained for the transitions from both valleys.[21]

IV. CONCLUSIONS

Summarizing, a simple model for the calculation of the quantized states of electrons and holes confined in lead-salt QW's has been presented here. It has been solved analytically and gives a good description of the quantum size effect observed in various PbTe QW's. It also provides simple eigenfunctions allowing the calculation of the complete optical spectra. The lifting of the valley and of the spin degeneracy of the electronic states in lead-salt QW's due to the quantum size effect was explained and limitations of the parabolic approximation were made clear, especially in the description of the temperature dependence of the transition energies.

The Rashba spin-orbit term in the effective Hamiltonian for electrons and holes in lead-salt QW's [Eqs. (4) and (6)] has been derived. The fabrication of asymmetric PbTe QW's and the study of their optical spectra would be of great interest. The spin splitting in such QW's derives exclusively from the mesoscopic asymmetry once the lead salts, contrary to the III-V compounds, present microscopic inversion symmetry. The study of this fine structure in the electronic structure of asymmetric lead-salt QW's would permit a more stringent test of both theoretical and experimental methods.

To conclude, we find that the results presented here give enough ground to believe that the model introduced can be of great help in planning the experiments and in the fabrication of devices based on the quantum confinement effect in lead-salt QW's. In particular, it can be useful in the study of the electronic effects in the magnetic and transport properties of these QW's as well as in the physics of other lead-salt nanostructures, like quantum wires and quantum dots.

ACKNOWLEDGMENTS

This research has been supported by FAPESP and CNPq, Brazil. Many thanks go also to Professor F. Beltram and Professor G. La Rocca for discussions, to Professor R. Kishore and Professor E. Abramof for a critical reading of the manuscript, and to Professor F. Bassani and Scuola Normale Superiore di Pisa, where part of this work was done, for the kind hospitality.

[1] R. Dalven, in *Solid State Physics: Advances in Research and Applications*, edited by F. Seitz, D. Turnbull, and H. Ehrenreich (Academic, New York, 1973), Vol. 28, p. 179.
[2] F. Geist, W. Herbst, C. Mejia-Garcia, H. Pascher, R. Rupprecht, Y. Ueta, G. Springholz, G. Bauer, and M. Tacke, Phys. Rev. B **56**, 13 042 (1997).
[3] D. L. Partin, Semicond. Semimet. **33**, 311 (1991).
[4] A. Ishida, S. Matsuura, M. Mizuno, and H. Fujiyasu, Appl. Phys. Lett. **51**, 478 (1987).
[5] S. Yuan, G. Springholz, G. Bauer, and M. Kriechbaum, Phys. Rev. B **49**, 5476 (1994).
[6] W. Goltsos, J. Nakahara, A. V. Nurmikko, and D. L. Partin, Appl. Phys. Lett. **46**, 1173 (1985).
[7] M. V. Valeiko, I. I. Zasavitskii, A. V. Matveenko, B. N. Matsonashvili, and Z. Rukhadze, Superlattices Microstruct. **9**, 195 (1991).
[8] I. I. Zasavitskii, E. V. Bushuev, S. O. Ferreira, P. Motisuke, and I. N. Bandeira, Superlatt. Microstruct. **25**, 505 (1999).
[9] M. Kriechbaum, K. E. Ambrosh, E. J. Fantner, H. Clemens, and G. Bauer, Phys. Rev. B **30**, 3394 (1984); M. Kriechbaum, P. Kocevar, H. Pascher, and G. Bauer, IEEE J. Quantum Electron. **24**, 1727 (1988).
[10] See, for instance, J. O. Dimmock, in *The Physics of Semimetals and Narrow Gap Semiconductors*, edited by D. L. Carter and R. T. Bate (Pergamon, New York, 1971), p. 319.
[11] R. E. Doezema and H. D. Drew, Phys. Rev. Lett. **57**, 762 (1986).
[12] M. Zaluzny, Phys. Rev. B **39**, 12 948 (1989).
[13] G. Bastard, *Wave Mechanics Applied to Semiconductor Heterostructures* (Les Editions de Physique, Les Ulis, 1990).
[14] E. A. de Andrada e Silva, G. C. La Rocca, and F. Bassani, Phys. Rev. B **55**, 16 293 (1997).
[15] V. Korenman and H. D. Drew, Phys. Rev. B **35**, 6446 (1987); V. K. Dugaev and P. P. Petrov, Phys. Status Solidi B **184**, 347 (1994).

[16] C. R. Hewes, M. S. Adler, and S. D. Senturia, Phys. Rev. B **7**, 5195 (1973).

[17] M. de Dios Leyva and J. Lopez-Gondar, Phys. Status Solidi B **138**, 253 (1986).

[18] F. Stern and W. E. Howard, Phys. Rev. **163**, 816 (1967).

[19] L. V. Keldysh, Phys. Status Solidi A **164**, 3 (1997).

[20] In all the results shown here we have used the effective masses listed in Table I and the following composition and temperature dependent energy gaps determined experimentally, $E_g(x,T) = 189.7 - 543x + 0.45T^2/(T+50)$ meV (see, for instance, the Landolt-Börnstein New Series tables) for $Pb_{1-x}Sn_xTe$ and $E_g(x,T) = 189.7 + 0.48T^2[(1-7.56x)/(T+29)] + x4480$ meV [S. Yuan, H. Krenn, G. Springholz, and G. Bauer, Phys. Rev. B **47**, 7213 (1993)] for $Pb_{1-x}Eu_xTe$.

[21] P. Rappl, Y. Ueta, E. Abramof, E. A. de Andrada e Silva, L. Dellamore, and F. Beltram (unpublished).

[22] G. Springholz, G. Ihninger, G. Bauer, M. M. Olver, J. Z. Pastalan, S. Romaine, and B. B. Goldberg, Appl. Phys. Lett. **63**, 2908 (1993).

[23] S. Yuan, H. Krenn, G. Springholz, Y. Ueta, G. Bauer, and P. J. McCann, Phys. Rev. B **55**, 4607 (1997).